Nonlinear Ultrafast Optics

By Omri Atir & Eliran Shishportish (Instructor: Mai Tal)

Abstract

In this paper we will present and discuss the phenomenon of SHG – Second Harmonic Generation, which lies in the vast field of nonlinear optics. To do so, we used class 4 laser – MIRA900 femtosecond laser, and optical system that directs its beam into Barium Borate (BBO) crystal. By theory explained in the introduction part, we expect that the incident laser frequency will be doubled (wavelength will be divided by two) when exiting the crystal. To validate that expectation, First, we measured the laser properties especially its wavelength spectrum and its peak that represented its fundamental wavelength. We found out that $\lambda_{FF} = 794.419\ [nm]$. Second, we after system configuration we measured the output beam and found out that $\lambda_{SH} = 397.080\ [nm]$. Later we conducted a numerical simulation to show the connection between SHG intensity and incident beam angle. Lastly, we measured that dependency and extracted crystal thickness $L_0 = 2.388 \cdot 10^{-4}$ [m] and compared it with our simulations.

1) Introduction

Nonlinear optics (NLO) is the branch of optics that describes the behavior of light in nonlinear media, which means media that the polarization density **P** responds non-linearly to external electric field **E** of the light [1]. The Typical way that nonlinear optics phenomena occur is when highly intense laser interact with such media. The beginning of the field is often marked as the discovery of Second harmonic generation (SHG) by Peter Franken in 1961 [2]. Today nonlinear optics have many applications that impact daily life, including telecommunications, commercial lasers, sensors, medicine, quantum optics and many more [3].

In this experiment we will focus on the SHG process. This is a process which two photons with same frequency interact in a nonlinear media and "combined" into one photon with a doubled frequency and energy [4].

Theoretical Background

The main change between classical optics and nonlinear optics is the presence of nonlinear response of the polarization vector to the photon's electrical field. We can treat the nonlinear response as infinite power series in **E** strength, such that:

$$(1)\ \tilde{\boldsymbol{P}}(t) = \epsilon_0\left(\chi^{(1)}\tilde{\boldsymbol{E}}(t) + \chi^{(2)}\tilde{\boldsymbol{E}}^2(t) + \chi^{(3)}\tilde{\boldsymbol{E}}^3(t) + \cdots\right)$$

Where upper tilde (~) sign refers to time dependent quantities, $\chi^{(n)}$ is the n'th order susceptibility and ϵ_0 is vacuum permittivity constant [1]. The SHG relate to the second term of the series, where it can be seen directly that when applying (strong enough) electric field, the polarization vector has contribution from second order magnitude of the field. Therefore, when we consider this and treat the polarization vector in the media as independent electric source (see supplementary section 1.1), the process generates electric field in the form of light with twice the initial frequency. In addition, big portion of the incident light wave interact linearly with the medium and come out unchanged. An illustration of the process is presented below:

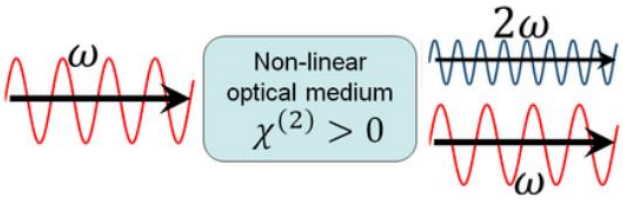

Figure (1)- SHG illustration [4].

To achieve such process with maximum efficiency, such that the output beam amplitude is maximal with the given laser condition, it is crucial to perform a "phase matching" process (see supplementary section 1.2). The relation between output beam intensity I_3 and the phase mismatch Δk is derived in Boyd -Nonlinear Optics, Third edition [2]:

$$(2)\ I_3 \propto L^2 sinc\left(\frac{\Delta k L}{2}\right)$$

Where L is the effective path length of the light inside the BBO crystal (exact formula in supplementary section 1.2 -eq 8). Each of the values is dependent in the incident angle of the laser with the

perpendicular direction to the surface of the crystal, that will be marked as - α.

3) Experimental Methods

a. Experimental System:

as stated in the abstract section, we used "MIRA900" femtosecond ultrafast laser as a beam source. To awake SHG phenomenon the laser tuned to approximately 8 nm in width and its peak centered around 794 nm. By spinning the ND wheel filter, we made sure the laser beam power does not go over 5 [mW] so that optical parts in the system, and the spectrometer, will not be damaged. The measurement of the power was made by mobile thermal power meter that placed in the beam's way. By mirrors, the beam directed the BBO crystals placed between two lenses. After that, the beam passed through dichroic mirror that reflected the fundamental frequency of the beam to a beam blocker and enable the second harmonic frequency to pass through it. At last, we measured the output spectrum by the spectrometer. (More details about experimental system found in supplementary section 2).

a schematic illustration of the system can be seen below:

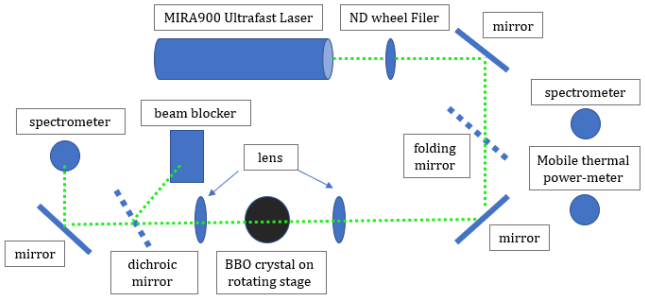

Figure (2)- optical experimental system.

The BBO crystal was mounted on rotating stage. That stage could be controlled manually or by MATLAB code, with precision of 0.1 milli degree. It is important to mention that the by manufacturing details, the crystal create maximum output intensity when the incident beam wavelength is [800nm] and its incident angle is zero.

b. Extracting Laser's Fundamental Frequency and Observing SHG:

The purpose of this stage was to measure laser's fundamental frequency – FF ,and observe at first time the SHG phenomenon. To do so, we made measurement using MATLAB automation code (see supplementary section 5) of the laser spectrum. Each spectrum measurement presented counts vs. wavelength [nm] at selected integration time. We used the spectrum extracted data to perform a gaussian fit and extracted the centered distribution wavelength of the laser (see supplementary section 3). After tuning the optical system, we observed and measured in the same process the SHG spectrum and extracted its center distribution wavelength.

The results we got are:

$$\lambda_{FF} = 794.419 \pm 0.028\ [nm], \qquad 0.0035\%\ error$$

$$\lambda_{SH} = 397.080 \pm 0.030\ [nm]\,, \qquad 0.0076\%\ error$$

$$\frac{\lambda_{FF}}{\lambda_{SH}} = 2.00065 \pm 1.6 \cdot 10^{-4}$$

Which with precision up to 3 digits after decimal point, as expected in theory.

c. Phase Matching Simulation

This part was made for preparation to our upcoming actual lab measurements. In this section we wrote numerical simulation in python code to simulate the relation between the incident angle of the beam with the crystal – α and the SHG expected intensity. This relation based on eq.2 and fully developed in supplementary section 4. This numerical simulation allowed us to observe the general behavior of the phase matching dependency with incident angle and with different crystal lengths.

d. SHG Intensity Measurements and Extracting Crystal Length.

In this section, we wanted to confirm the relation written in eq. 2, and extract crystal length L_0. To do so, first we wanted the check the physical alignment of the stage with the incident beam. We know that when the beam has incident α angle of zero, we should get maximum SHG. When the system was tuned, we semi - manually scanned the angle range, using MATLAB functionality described in supplementary section 5, while checking real time spectrum using "Oceanview" software (see supplementary section 2, spectrometer details). We found that the maximum intensity of the second harmonic is when the motor is around 7.5 degrees. Then we defined the motor an angle range of 4 to 11 degrees and conducted automated measurements using the parameters: integration time = 100 [ms], jump = 0.05 degree, burst number = 30. Unfortunately, the laser exited mode – locking and SHG stopped around 7.9 degrees, so the data was valid only within 4 – 7.9 degrees angle range. The data collected for each angle, was averaged and a gaussian fitting were made to find SHG intensity (see

supplementary section 6) and their standard deviation. Lastly, we found the maximum I-SHG of all calculated maximums, and its matching angle, and shifted all angles by that angle such that I-SHG will be at angle zero, and all other points will be centered in related to it. This should eliminate the factors that made shift in the graph like system misalignment and difference of incident wavelength with 800 [nm]. Also, we normalized all the other maximums by I-SHG value. We decided to normalize the data and extract L_0 only by inner sinc dependance. We did that because we assumed that not every photon that interacts with the detector is counted. This affects the scale of the data that also depends on L_0^2. Therefore, there is unnecessary constrains that we want to exclude.

As explained in the theoretical background, eq. 2 describe the relation between second harmonic intensity – I_{SH}, with phase matching parameter Δk and effective optical length of the beam inside the crystal L. In the supplementary section 3 eq. 12 we developed the full relation between I_{SH} and incident angle α. Based on that relation we fitted the data according to the following normalized formula:

$$(3)\quad I_{SH-normalized} = sinc^2\left(\frac{2\pi a_0}{\lambda_{FF}\sqrt{1-\frac{\sin^2(\alpha-a_1)}{n_0^2(\omega)}}}\left(n_0(\omega) - \left(\frac{sin^2\left(\theta_0+\sin^{-1}\left(\frac{\sin(\alpha-a_1)}{n_0(\omega)}\right)\right)}{\bar{n}_e^2(2\omega)}+\frac{\cos^2\left(\theta_0+\sin^{-1}\left(\frac{\sin(\alpha-a_1)}{n_0(\omega)}\right)\right)}{n_o^2(2\omega)}\right)^{-\frac{1}{2}}\right)\right)+a_2$$

Where a_0 represent L_0 the thickness of the crystal, a_1 represent built in angle shift, a_3 represent free parameter to add more degrees of freedom to the fit. The error analysis of $I_{SH-normalized}$ and α is fully presented in supplementary section 6.

3) Results

a. simulation results.

According to supplementary section 4 detailed steps, we chose to simulate five graphes of normalized I-SH (meaning we discarded outer coefficent multipling the squared sinc) as function of incident angle α. Each graph with different L_0 vaule within the range 0.01 to 100 [mm]. The results are presented below:

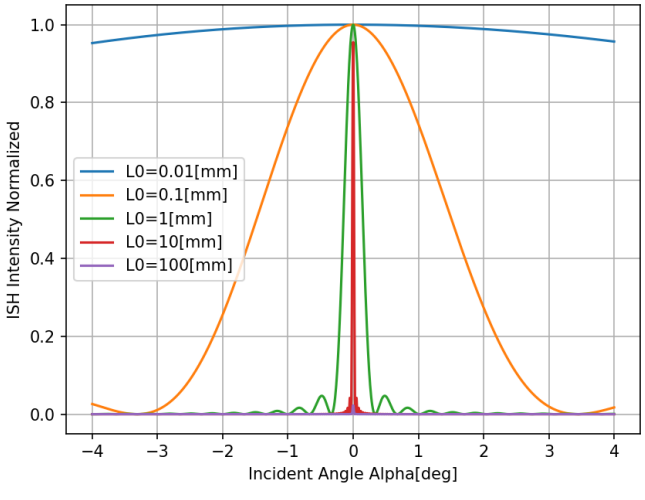

Figure (3) - $I_{SHG}(\alpha)$ numerical simulation

By observing simulation results, we can see that for greater crystal thickness, the sinc squared is narrowerer. Also, for thinner crystals the peak is flatter and the secondary peaks is also wider. This results is not surprising and can be explained by physical theory. Lets assume the phase mismatch Δk has small value close to zero. Greater L_0 value means that when the incidnt waves and the building up output wave propagating through the crystal, the phase mismatch will ocurr on longer distance. Therefore the destructive interfirence will be more powerful such that even small mismatch will land the output SHG intensity. Within thiner crystals, the propagating process will be short, leaving no segnificant impact on output intensity.

b. phase matching results.

The fit that we got according to eq. 3 were:

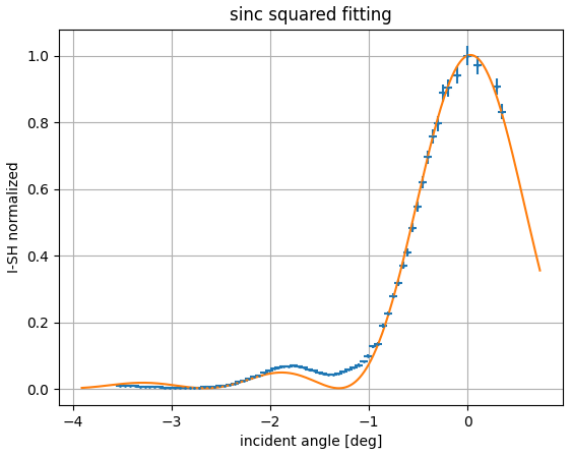

Figure (4) - $I_{SHG-normalized}(\alpha)$ lab measurements.

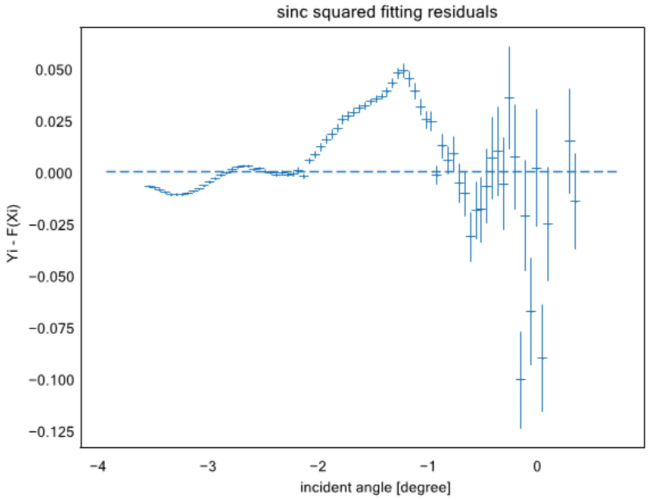

Figure (5) - $I_{SHG-normalized}(\alpha)$ residuals.

Parameter	Value	Relative error
χ^2_{red}	23	-
p_{val}	0	-
a_0 [m]	$2.541 \cdot 10^{-4} \pm 6.2 \cdot 10^{-6}$	2.4%
a_1 [deg]	$-3.7 \cdot 10^{-4} \pm 9.1 \cdot 10^{-4}$	250%
a_2	0.0022 ± 0.0013	63%

Table (1) – fitting parameters for $I_{SHG}(\alpha)$.

Fit quality parameters are not in the desired range. However, the fit seems to match the data aroud the main peak. The residuals showing a rising distance of the data in the first downfall after the main peak. By that facts we can say that the fit was unsuccessful. Therefore we conducted another fit of the sinc without secondary peaks. The fit and analyis presented in supplementary section 7. The extracted value of L_0:

$$L_0 = 2.541 \cdot 10^{-4} \pm 6.2 \cdot 10^{-6}\ [m]\ \ ,2.4\%\ error$$

and the value that we got from the second fitting:

$$L_0 = 2.388 \cdot 10^{-4} \pm 4.1 \cdot 10^{-6}\ [m]\ \ ,1.7\%\ error$$

We did not have the theoretical value of L_0 but when comparing the fitting with the simulation results in fig. 3, we can say that the data and the fitting is seems in the same scale of sinc width for value of L_0 in the order of 10^{-4} [m], the same order of L_0 we extracted in our fitting.

4) Discussion and conclusions

In this study, we established an experimental setup to observe second harmonic generation (SHG) and conducted various measurements to analyze its behavior and properties.

Laser fundamental wavelength. In this part we directly measured the laser's spectrum and SHG spectrum. We found that λ_{FF} equal twice of λ_{SHG} with large (up to three decimal points) precision. By that result we can confirm strongly that the observed phenomenon was SHG as depicted in fig. 1.

SHG vs. incident angle. In this part, we wanted to confirm eq. 3 and extract crystal thickness L_0. According to our results which included only half of the pre-determined range, we got unsuccessful fit when taking in consideration all data points. We can see that the inconsistency of the fit with the data is in areas where I_{SHG} gets low values. This fact can be explained by the background noise in measurements that gets more impact when we measure low values of I_{SHG}. When fitted data only around main peak to minimize background noise, we got better fit in terms of fit quality parameters (see supplementary section 7).

We believe that if we had measured all planned angle range, we would get more accurate and credible results.

In conclusion we expanded our knowledge about nonlinear optics, and specifically SHG phenomenon. We developed our experimental skills and developed appreciation for research in this field of study.

5) References

[1] Wikipedia. Nonlinear Optics url: https://en.wikipedia.org/wiki/Nonlinear_optics

[2] Boyd, Robert W. *Nonlinear optics*. Academic press, 1992. Pages 1-10, 69-84.

[3] Ali, Owais. "What is Nonlinear Optics?". AZoOptics. 13 June 2023. https://www.azooptics.com/Article.aspx?ArticleID=2406

[4] Wikipedia. Second Harmonic Generation url: https://en.wikipedia.org/wiki/Second-harmonic_generation